D. Fan
Research Fellow,
Department of Civil Engineering,
The University,
Dundee DD1 4HN
Scotland, U.K.

A. Tijsseling
Research Officer,
Department of Civil Engineering,
Delft University of Technology,
2600 GA Delft,
The Netherlands

Fluid-Structure Interaction With Cavitation in Transient Pipe Flows

The interactions between axial wave propagation and transient cavitation in a closed pipe are studied. Definitive experimental results of the phenomenon are produced in a novel apparatus. The apparatus is characterized by its simplicity and its capability of studying transient phenomena in a predictable sequence. The influence due to friction is small and the representations of the boundary conditions are straightforward. Measurements with different severity of cavitation are provided to enable other researchers in the area to compare with their theoretical models. A new cavitating fluid/structure interaction cavitation model is proposed. The measurements are compared with the column separation model of Tijsseling and Lavooij (1989) and the new model to validate the experimental results.

Introduction

Transient cavitation frequently occurs in liquid-filled pipelines in unsteady flow regions. It is a local phenomenon which develops wherever the fluid pressure drops to the vapor pressure. In fully-filled piping systems, transient cavitation is normally characterized by two flow regimes. In a distributed cavitation region, vapor bubbles are dispersed amongst the liquid. In a column separation region, the bubble population is sufficiently large to coalesce to form a vapor pocket within the pipe.

Most of the work on transient cavitation deals with pressure wave propagation in rigidly anchored pipelines. The flexibility effects of the pipewalls are taken into account by reducing the fluid wavespeed (Chaudhry, 1979). For distributed cavitation, authors such as Kranenburg (1974) and Martin et al. (1976) find that the Lax-Wendroff scheme is applicable for implicit treatment of shock waves. For cavitations which last longer than 1.5 seconds, Zielke et al. (1989) find that gas release effects should be taken into account. For vaporous cavitation, Provoost (1976) and Kot and Youngdahl (1978) find that the concentrated (discrete) cavity model is suitable for most applications. Fox and McGarry (1983) have developed a model which includes thermodynamic effects due to heat transfer between liquid and cavities. They found that the thermodynamic effects are important for liquids with large vapor pressure like propane or butane.

In practice, most pipelines are not rigidly anchored. In such cases. the flexibility of the pipewalls not only results in reduced fluid wavespeed but also in the presence of stress waves within the pipewalls. The dynamics of such a pipe system is therefore analogous to that of a structural frame coupled with the dynamics of the fluid. Wilkinson (1978), Wiggert et al. (1985, 1987) and Lavooij and Tijsseling (1989) have all proposed a variety of analytical and numerical methods to predict the coupled dynamic response of piping systems. In general, the dynamics of a pipework is influenced by four wave families: axial, flexural and torsional waves in the pipewall and pressure waves in the fluid. They coexist during transience and have different degrees of influence on transient cavitation.

Axial waves in the pipewall can induce negative fluid pressures upon reflection or transmission at geometrical discontinuities. In addition, radial expansion of the pipewall associated with compressive axial stress waves can also be sufficient to induce cavitation. If friction and cross-sectional flows are neglected, flexural and torsional waves cannot induce pressure changes at wavefronts. However, they can induce axial waves and hence cavitation when reflected at boundaries (e.g., at elbow and tee junctions). In most recent studies on fluid/structure interaction without cavitation, it is shown that the phenomenon can result in significant increases of peak pressures and significant reduction of natural frequencies of pipework (Tijsseling and Lavooij, 1990; Wiggert et al., 1987; and Wilkinson, 1978).

Although there is no lack of literature on fluid/structure interaction or transient cavitation, the work on both subjects is scarce. Schwirian (1982) developed a Finite Element technique which can model multidimensional fluid/structure interaction problems with cavitation. Tijsseling and Lavooij (1989) proposed a column separation—fluid/structure interaction model for piping systems. Their work is only applicable for column separation in a typical reservoir-pipe-valve system, and no validation results were given. In practice, distributed cavitation frequently accompanies column separation in low pressure regions during transience. This results in regions of reduced fluid wavespeed rather than a separated cavity as in the case of column separation. The additional effects due to the reduction of fluid wavespeed therefore must be taken into account in a comprehensive analysis.

Experimental Method

Accurate experimental measurements of transient cavitation in a closed tube are obtained. The apparatus consists of a slightly pressurized steel tube suspended by two long thin steel wires. Transients in the pipe are produced by impacting a solid steel rod onto one end of the pipe (Fig. 1). This method of

Contributed by the Fluids Engineering Division for publication in the JOURNAL OF FLUIDS ENGINEERING. Manuscript received by the Fluids Engineering Division September 13, 1990. Associate Technical Editor: E. Michaelides.

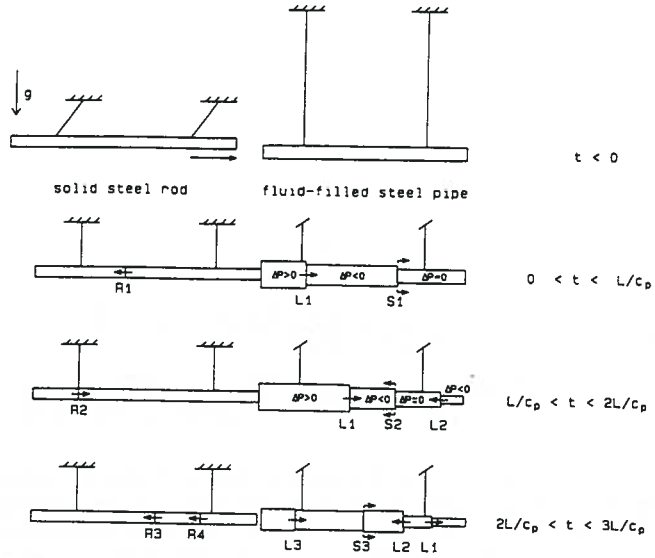

Fig. 1 Sequence of events in the apparatus

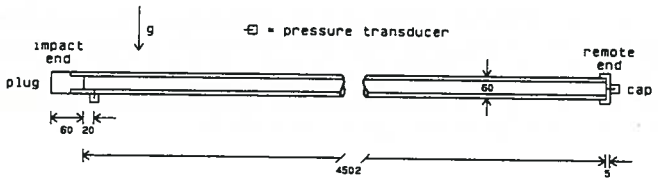

Fig. 2 End pieces

Table 1 Properties of the apparatus

Item	Method of measurement	Instrument Standard Accuracy	Deviation	Value	Unit
PIPE					
Young's modulus	Uniaxial compression test on a 200 mm long specimen			168±5	GN/m²
Poisson's ratio	Uniaxial compression test on a 200 mm long specimen			0.29±0.01	
Steel mass density	Micrometer, and weight a 200 mm long specimen	2.0	5.0	7985±7	kg/m³
Internal diameter	Direct measurement : micrometer	0.03	0.1	52.02±0.13	mm
External diameter	Direct measurement : micrometer	0.003	0.020	59.91±0.02	mm
Internal length	Direct measurement : tape measure	0.5	0.5	4502±1	mm
ROD					
Young's modulus	Uniaxial compression test on a 200 mm long section			200±6	GN/m²
Mass density	Micrometer and weight a 200 mm long section	4.0	0.0	7848±4	kg/m³
Diameter	Direct measurement : micrometer	0.01	0.04	50.74±0.05	mm
Length	Tape measure : include curvature at the impact end	0.5	0.5	5006±1	mm
END PIECES					
Mass of end plug	Direct = electronic scale			1.2866	kg
Mass of end cap	Direct = electronic scale			0.2925	kg
FLUID (assumed values)					
Water mass density				999	kg/m³
Water bulk modulus				2.14	GN/m²
Darcy-Weisbach friction factor				0.01	
Vapour pressure				0.02	bar

generating fluid transients by structural impact was developed by Vardy and Fan (1986, 1987) to study fluid/structure interactions in noncavitating flows. The method has the advantages of minimizing complications due to steady state-pressure gradients associated with friction and gravity. The boundary conditions can be modeled accurately, thus allowing the particular effect (and in this case the interactions between axial waves and vapor cavities) to be studied with confidence. Flexural and torsional effects are not introduced for the present application.

Sequence of Events. When the experiments commence, the rod is released from the raised position. It accelerates under the influence of gravity until it reaches its lowest position. At the instant of impact, two sets of wavefronts are generated in the pipe which travel along the fluid and the pipewall. In cases without cavitation, the wavespeed in the pipewall is about 3.4 times faster than in the fluids. Interactions exist between the pipewall and the fluid at the wavefronts due to Poisson ratio effects (Poisson coupling). At the stress wavefront S1, this produces a slight drop in the fluid pressure which is followed by an increase in pressure due to the pressure wavefront L1 (Fig. 1).

As the stress wavefront S1 reaches the remote end of the pipe, it pushes the closed end away from the fluid. This induces a large rarefraction wavefront L2. In cases without cavitation, the magnitude of L2 can be double that of the initial pressure rise due to L1. During the first $2L/c_p(\approx 2$ ms) after impact, the rod remains in contact with the pipe. The rod is deliberately chosen to be longer than the pipe such that the reflected wavefront in the rod (R2) cannot reach the impact end before S2 does. At $t=2L/c_p$, the tensile stress wavefront S2 reaches the impact end and separates the rod from the pipe. The impact end becomes free and no multiple impact occurs. Therefore, the rod can be regarded as semi-infinite in the calculations. By varying the amount of initial pressure in the pipe, cavitation can be initiated either at the remote end (column separation) or at the stress wavefront S1 due to Poisson coupling effects (distributed cavitation). The time-scale of the experiments is in milliseconds and so the relatively slow effects due to gas release are insignificant (Zielke et al., 1989).

Cavitation Severity Index. A numerical index has been pro-

Nomenclature

A = cross-sectional area
c = wavespeed, defined in Wiggert et al. (1985)
f = Darcy-Weisbach friction factor
g = gravitational acceleration
G_f, G_p = Poisson coupling factors, defined in Wiggert et al. (1985)
L1–3 = liquid wavefronts
L = internal length
p = fluid pressure
R1–4 = axial stress wavefronts in the rod
R_H = hydraulic radius
S1–3 = axial stress wavefronts in the pipewall
S = cavitation severity index
t = time
T_c = duration of the first column separation at the remote end
U = axial velocity
w = self weight terms, defined in Vardy and Fan (1987)
ρ = mass density
σ = axial stress in pipewall
τ = shearing stress in fluid = $f\rho_f(U_f-U_p)\lvert U_f-U_p\rvert/2$
$\forall$ = cavity volume

Subscripts

f = fluid
p = pipewall
r = rod

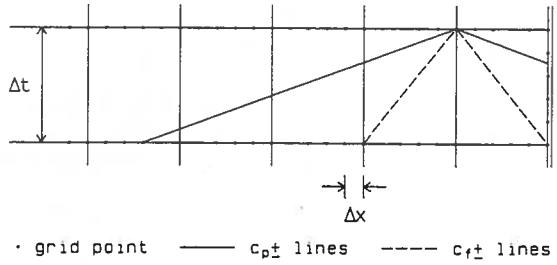

Fig. 3 Numerical grid

posed by Martin (1983) to classify the severity of cavitation in rigidly anchored pipelines. It is proportional to the fluid wavespeed and the duration of column separation. In cavitating fluid/structure interaction flows, the phenomenon is dominated by stress wave propagation in the pipewall. A similar severity index, which is based on the axial stress wavespeed, is chosen for the present study:

$$S=\frac{T_c}{(2L/c_p)} \tag{1}$$

where T_c is the duration of the first vapor cavity at the remote end. In the present apparatus, for cases where $S<1.5$, the situation is classified as slight. For cases where $S>2.5$, the situation is classified as severe. The intermediate cases are classified as moderate.

Details of the Apparatus. The pipe is 4.5 m long (316L stainless steel 2 in. NB 40s) and it is sealed by two end pieces (Fig. 2). Prior to the test runs, the pipe is filled with ordinary tap water and inclined to a vertical position. A mallet is used to tap the pipe to encourage the air bubbles attached on the pipewall to rise. A screw valve is located at the top of the pipe to bleed the air into the atmosphere. This process is repeated several times until there is negligible amount of air pocket left in the pipe. The fluid is then pressurized to the desired initial pressure by using a hand pump and a calibrated manometer.

The apparatus is extensively instrumented with pressure transducers (Kistler 7031), strain gauges, accelerometers (PCB 305A05), a laser Doppler vibrometer and a high speed video camera (Kodak Ektapro 1000). All instruments are connected to a high speed data acquisition system which has sixteen channels, each capable of taking 125,000 samples per second. Fluid pressure, structural displacement, velocity, acceleration and strain of the pipe and the rod have been measured. In this paper only a few of the measured results are selected for concise presentation. The laser and the video camera measurements are used to determine the rod impact velocity. The pressure measurements are used to study the interactions between axial wave propagations and vapor cavities.

The physical and material properties of the apparatus are presented in Table 1. All important parameters are measured, such that the theoretical and the experimental results can be assessed independently. The only parameter that needs to be inferred from the measurements is the initial pressure within the pipe. This is due to the thermal expansion of the fluid and the pipewall. As the apparatus is a closed tube, the volumetric changes associated with temperature changes can significantly influence the initial water pressure within the tube. The pressure change due to a typical daily temperature variation of 8°C can be as much as 1 MPa. The apparatus therefore behaves rather like a thermometer. In the theoretical simulations, the value of the initial pressure (measured by a manometer) is slightly adjusted such that the measured and the calculated cavitation levels at the remote end of the pipe are equal.

Repeatability of the Experiments. Five cases of results are presented, ranging from no cavitation ($S=0$) to Poisson coupling induced cavitation ($S=2.8$). There are three runs of experiments per test case, and the typical elapse time between each run is less than five minutes. The repeatability of the test cases is shown in Fig. 4. Two results from each test case are chosen randomly for inspection. In the case where there is no cavitation ($S=0$), the measurements are almost identical between different runs. In all cases the magnitude and the timing of the main pressure peaks are highly repeatable. As the severity of cavitation increases, only the smaller high frequency peaks become less repeatable. The level of repeatability is sufficient for our purpose. The present method of inducing cavitation produced sharper and more uniform excitations across the pipe cross section than those produced by valve closure.

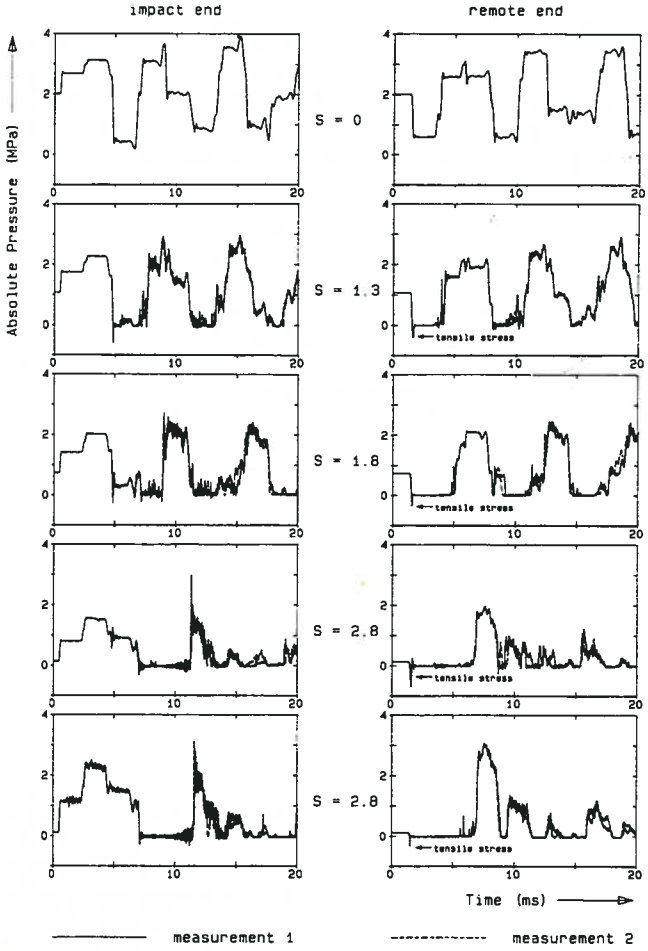

Fig. 4 Typical repeatability of pressure measurements in the apparatus

Theory

In the following analysis the theory assumes elastic pipewall material and straight thin-walled pipe geometry. Radial inertia of the pipewall is neglected so the phenomenon is nondispersive in the absence of cavitation. The free gas content in the liquid is assumed to be zero and no gas release or thermodynamic effects are included.

Governing Equations. A detailed discussion of the constitutive equations of axial wave propagations in transient pipe flows has been presented by Vardy and Fan (1987). The equations have been derived by considering the continuity, momentum and material relationship of the fluid and the pipewall. Similar expressions have also been found by Schwarz (1978) and Wiggert et al. (1985). The equations can be transformed by the Method of Characteristics to yield the following four compatibility equations which are valid along the characteristic directions:

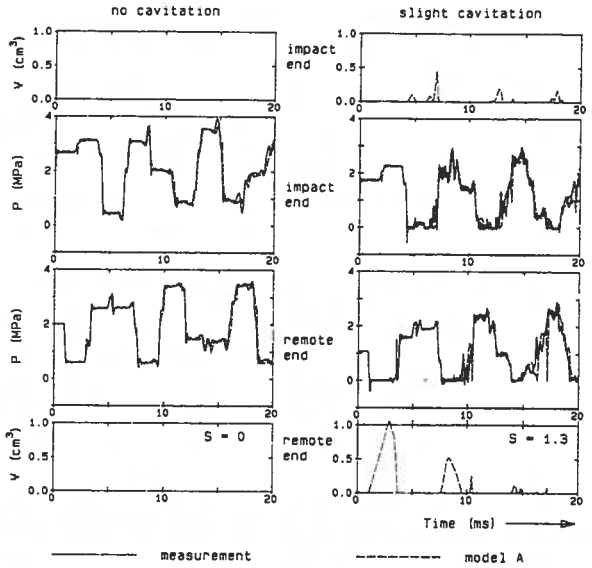

Fig. 5 None and slight cavitation: model A

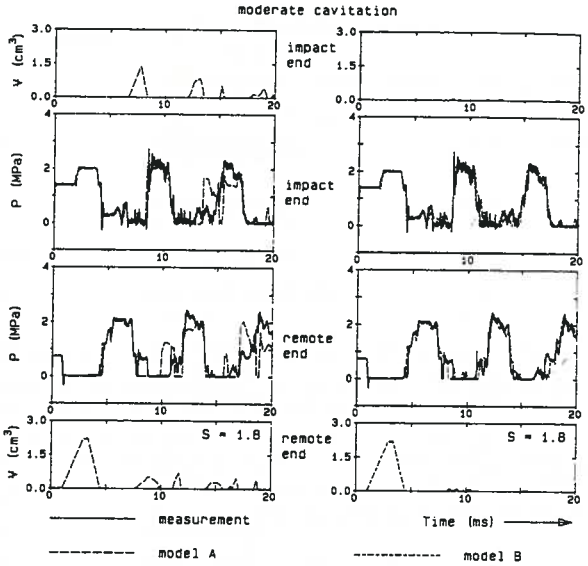

Fig. 6 Moderate cavitation: model A and model B

Fluid (along $dx/dt = \pm c_f$):

$$\frac{dp}{dt} \pm \rho_f c_f \frac{dU_f}{dt} - G_f\left(\frac{d\sigma_x}{dt} \mp \rho_p c_f \frac{dU_p}{dt}\right) = \mp c_f\left\{\left(\frac{\tau}{R_H} + w_f\right) - G_f\left(\frac{\tau}{R_H}\frac{A_f}{A_p} + w_p\right)\right\} \quad (2)$$

Pipe (along $dx/dt = \pm c_p$):

$$\frac{d\sigma_x}{dt} \mp \rho_p c_p \frac{dU_p}{dt} - \frac{1}{G_p}\left(\frac{dp}{dt} \pm \rho_f c_p \frac{dU_f}{dt}\right) = \mp c_p\left\{\left(+\frac{\tau}{R_H}\frac{A_f}{A_p} + w_p\right) - \frac{1}{G_p}\left(\frac{\tau}{R_H} + w_f\right)\right\} \quad (3)$$

The equations relate four unknowns, namely, the axial stress σ, pipe velocity U_p, pressure p, and fluid velocity U_f. The first two terms in the equations constitute the decoupled compatibility equations for axial waves in both media. The last two terms include Poisson ratio effects due to radial flexibility of the pipewall. The full expressions of the wavespeeds (c_f, c_p) and the Poisson coupling factors (G_f, G_p) are given by Wiggert et al. (1985). The solutions of the equations have been validated against experimental data as well as other methods of solving the constitutive equations (e.g., Lavooij and Tijsseling, 1989 and Wiggert et al., 1985).

In the cavitation regions, the concentrated cavity model by Streeter (1969) and Provoost (1976) is adopted for the present application. This model is preferred above others because of its ability to predict most vaporous cavitation situations. The model is also simple to implement and gives sufficiently accurate results. In the present application, the numerical oscillations reported by Provoost (1976) and Wylie (1984) have not been found. Therefore free gas pockets, like those used by the above authors to suppress numerical pressure spikes, are not necessary in the present model. The model concentrates the presence of vapor cavities at numerical grid points and thus allows the fluid wavespeed to remain constant in the intervening spaces. When an overpressure wave transverses a cavity, first it has to cause the cavity to collapse. The delay action associated with this behavior emulates the reduction of fluid wavespeed and its dependency on the void fraction. If a vapor cavity exists, the pipe axial stress and velocity are assumed to be the same across the cavity. In addition, the pressure in the cavity is assumed to stay constant at the vapor pressure level (Table 1).

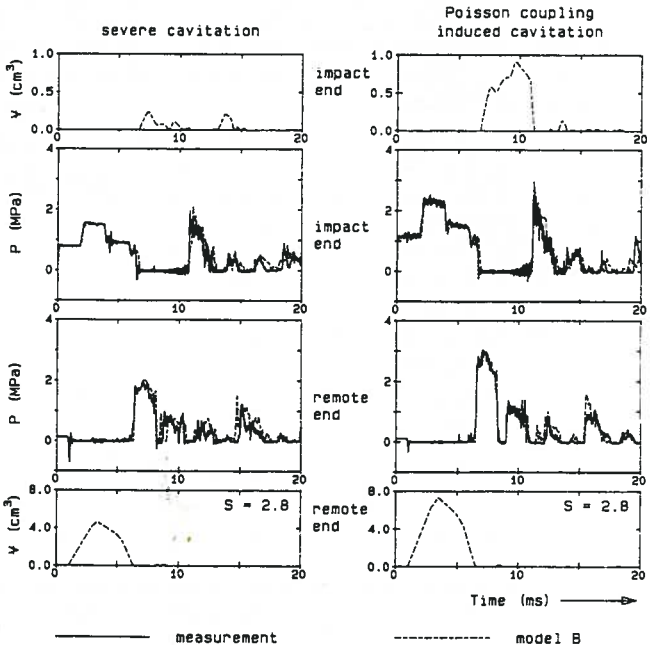

Fig. 7 Severe and Poisson coupling induced cavitation: model B

Solution Procedure. The numerical grid proposed by Tijsseling and Lavooij (1989) is adopted for the present application (Fig. 3). In their analysis, the characteristic lines are allowed to span several grid lengths and the wavespeeds are slightly adjusted such that interpolations are necessary only at the points near a boundary. In the absence of cavitation, Eqs. (2) and (3) are used to obtain the values of the four unknowns at the new time level. In cases where the pressure falls below the vapor pressure, Eqs. (2) and (3) are solved simultaneously with the vapor pressure to obtain the solution. The solution of these equations yields the fluid velocities on both sides of a vapor cavity at the grid point. These values are used to obtain the new cavity volume using the following relationship:

$$\forall_{NEW} = \forall_{OLD} + A_f(U_{fR} - U_{fL})\Delta t \quad (4)$$

where U_{fL} and U_{fR} are the fluid velocities on the left and the right hand side of the cavity respectively. A similar approach is also used for the transitory case of a collapsing cavity by solving Eqs. (2)–(5) simultaneously:

$$\forall_{NEW} = 0 \tag{5}$$

Boundary Conditions. At a boundary, only two characteristic lines are available and two boundary conditions must be used to obtain all the equations required.

(*a*) Impact end: For $0 \le t \le 2L/c_p$, the equilibrium and continuity relationships are:

$$\sigma A_p - pA_f = \sigma_r A_r$$
$$U_p = U_f = U_r$$
$$\sigma_r = \rho_r c_r (U_r - U_{ro}) \tag{6}$$

where U_{ro} is the initial velocity of the rod before impact and the subscript r denotes quantities related to the rod. The rod axis is in the same direction as the pipe axis. Note that the rod is simulated as a semi-infinite boundary because $2L_r/c_r$ is greater than $2L/c_p$.

(*b*) Remote (free) end: In the absence of a vapor cavity, the equilibrium and continuity equations are:

$$pA_f - \sigma A_p = 0$$
$$U_f = U_p \tag{7}$$

With column separation, the equilibrium relationship is still valid but the continuity equation is replaced by Eq. (8):

$$\forall_{NEW} = \forall_{OLD} + A_f(U_p - U_f)\Delta t \tag{8}$$

where $\forall_{OLD}$ and $\forall_{NEW}$ denote the cavity volume on the old and new time level respectively. This procedure is also used for the impact end in the presence of cavitation.

Results

The measurements from five different sets of experiments with increasing severity of cavitation are presented. The first two sets of measurements are compared with the column separation—fluid/structure interaction model (designated model A) by Tijsseling and Lavooij. Column separations at both ends of the pipe are modeled and no distributed cavitation effects are included. In the last two sets of experiments, the measurements are compared with the proposed cavitating fluid/structure interaction model (designated model B). In the intermediate case, the measurements are compared with both models. The rod impact velocity is 0.739 m/s in the first four cases, and is increased to 1.122 m/s in the last case.

In Figs. 5–7, the upper and lower graphs depict the calculated cavity volumes at the impact and the remote end of the pipe respectively. The duration of the first cavity formed at the remote end is used to calculate the cavitation severity parameter. In each figure, the continuous lines depict the measurements and the broken lines depict the numerical results from either model A or model B. In all simulations, the number of grid lengths in the pipe is 150. The $c_f \pm$ characteristic lines span five grid lengths, and the $c_p \pm$ characteristic lines span seventeen grid lengths (Fig. 3). This implies the time step is 0.11 milliseconds.

No Cavitation. In the absence of cavitation the minimum transient pressure in the pipe is about 1.8 MPa below the initial pressure (Fig. 5). The initial pressure in the pipe in this case is about 2 MPa. This pressure is sufficiently high to prevent cavitation and allow the experiment to be used as a control. It should be noted the pressure pattern of the present apparatus is very different from that of water hammer in a rigid pipeline (e.g., a reservoir-pipe-valve case: Chaudhry, 1979). The repetitive pressure pattern every $4L/c_f$ no longer exists. This is due to the presence of axial stress wavefronts which generate pressure changes at the wavefronts (Poisson coupling) and additional pressure waves when reflected at the boundaries. This phenomenon is not restricted to the present apparatus and it exists to some degree in all nonrigidly anchored pipelines. A related point of interest is that the initial pressure rise at the impact end is about 0.6 MPa. When the stress wavefront S1 (Fig. 1) reflects at the remote end, the magnitude of the rarefaction wave (L2) produced is about 1.4 MPa—more than double the initial pressure rise. Models A and B both predict identical results in this case and the comparisons with the measurements are almost exact. The results are consistent with the previous work on the apparatus (Vardy and Fan, 1989).

Slight Cavitation. In the second set of experiments, the initial pressure is lowered to about 1.07 MPa. At the impact and the remote ends, it is no longer possible to reduce the pressure by -1.8 MPa and -1.4 MPa, respectively (Fig. 5). Cavitation first occurs at the remote end due to S1 and later, at about 4 millisecond, at the impact end due to L2. The cavities exist only when the pressure at the corresponding location drops to the vapor pressure, hence confirming the validity of the results. One particular interesting observation is that the occurrence of the vapor bubbles mainly alternates between the pipe ends. This effect is more apparent as the severity of cavitation increases (Fig. 7). The fluid therefore behaves like an elastic column slopping between the end cavities. Model A predicts the events with good accuracy. Thus it can be inferred that the phenomenon is column separation dominant.

At the impact end, extremely high frequencies exist in the pressure measurements. This is thought to be due to the location of the pressure transducer relative to the vapor cavity. The transducer is located at about 20 mm from the inner surface of the end plug (Fig. 2). It is a recognized phenomenon (Safwat, 1972) that a small amount of distributed cavitation normally exists in the vicinity of a column separation region. It is therefore conceivable that the random collapse of the small bubbles within the distributed cavitation region can cause the high frequency signals in the measurements. This seems to be a local effect and the signals cannot be observed further along the pipe. At the remote end, the same effect cannot occur because the transducer is mounted on the inner surface of the end cap. In order to filter out the oscillations at the sampling frequency (125 kHz), a Shuman numerical procedure (Vliegenthart, 1970) is used for the pressure measurements at the impact end in all cases.

Moderate Cavitation. In Fig. 6, the initial pressure in the pipe is about 0.73 MPa. Cavitation is also initiated at the remote end by reflection of the stress wavefront S1 (Fig. 1). On the left hand side, the measurements are compared with model A. It predicts the first pressure peak due to cavity collapse at both ends of the pipe with a high degree of accuracy. The agreement between experiment and theory then begins to deteriorate with time. By using model B, distributed cavitation is modeled, and the subsequent pressure peaks are now accurately predicted. It can be deduced that distributed cavities are present and they interact significantly with pressure wave propagation. The calculated results indicate that model A overestimates the first cavity volume at the impact end. It is probably due to the model attempts to lump the distributed cavities towards the impact end. It is worthwhile noting that the results resemble that of cavitation in a reservoir-pipe-valve case (Martin, 1983), with additional secondary pressure peaks between the major ones.

Severe Cavitation. In Fig. 7, two cases of results with different rod impact velocity are presented. The initial pressure in the pipe is atmospheric in both cases. On the left hand side (low velocity), the pressure pattern changes significantly from the previous case. The duration of the cavity at the remote end is 50 percent longer than in the previous case but the magnitude of the first pressure peak is about the same. The most noticeable difference is the subsequent pressure peaks become less significant compared with the first one. Other measurements up to 5 seconds have shown that the pressure rapidly diminished to zero after 20 milliseconds. The reduction

of pressure and stress levels in the pipe is therefore highly significant. Most of the wavefront energy is converted to the kinetic energy used for moving the pipe away from the impact end. Model B is capable of predicting the amplitude and the timing of the events very well. The discrepancies at time greater than 14 millisecond correspond to the decrease in repeatability of the measurements (Fig. 4).

Poisson Coupling Induced Cavitation. In this set of experiments, the rod impact velocity is increased in order to generate cavitation associated with radial expansion of the pipewall due to the compressive stress wave S1 (Fig. 1). This effect is illustrated by the pressure trace at the impact end. The pressure level no longer remains constant during the first 2 milliseconds ($2L/c_p$) as in all the previous cases. The variable pressure level is due to the growth and collapse of the bubbles associated with S1. After S1 transverses the pipe, the entire length of the pipe is dispersed with bubbles. The overpressure wave L1 has first to cause all the bubbles to disappear before it can transverse the pipe. When S1 reaches the remote end, the cavity formed exists for about the same duration as in the previous case, even though the impact velocity is higher. However, the peak pressure is about 1 MPa higher and the relative magnitude of the subsequent pressure peaks is lower. Therefore, the rate of convertion of wavefront energy to kinetic energy is higher than the previous case. The ability of model B to predict these events is excellent, even in the presence of cavitation caused by radial expansion of the pipewall.

Tensile Strength of Water. At a short time after impact, the compressive stress wavefront S1 (Fig. 1) reaches the remote end and pushes the end cap away from the water. The water can be seen to sustain tensile stresses of between 0.35 to 0.7 MPa up to 0.15 millisecond before column separation occurs (Fig. 4). No direct correlation between the initial pressure, the duration and the magnitude of the tensile stresses seems to exist. Other work in this area has shown that water can sustain tensions up to much higher magnitudes in steel tubes. Plesset (1969) and Trevena (1984) gave informative reviews on theoretical and experimental aspects of the subject respectively. Davies et al. (1955) have also used a similar apparatus and found that water has a maximum dynamic tensile strength of about 1 MPa on clean steel surface.

The present apparatus is not specially designed for measuring the transient tensile strength of water. Indeed, only ordinary tap water has been used with a standard industrial steel pipe. Therefore, the abundance of nuclei in water must have encouraged the vapor cavities to grow. It is envisaged that higher transient tensile stresses can be measured if the water is purified and if the pipe interior is smooth.

Further Work

In the present theoretical model distributed bubbles in the fluid are lumped at the grid points to form localized vapor cavities. Whenever a pressure wave intersects a localized cavity, the magnitude of the pressure wave is modified by the presence of the cavity. However, an axial stress wave does not change in magnitude when it passes through a localized cavity (Fig. 3). This procedure is exact if Poisson coupling is absent between the fluid and the pipewall. If Poisson coupling effects are significant, the secondary pressure waves associated with axial stress waves must be modified by the vapor cavities. For the cases considered the interactions between the secondary pressure (precursor) waves and the localized vapor cavities is small enough to allow reasonably accurate predicted results. A more rigorous and general approach would be to allow the $c_p \pm$ lines to span one grid length and the $c_f \pm$ lines extend back several timesteps.

In principle, the experimental technique is not restricted to single pipe systems. Different piping configurations can be achieved by assembling elbow and tee junctions onto the remote end of the main pipe. In planar networks, additional effects due to flexural wave propagations in the pipewall must be taken into account. Work has already begun on the multipipe systems with and without cavitation.

Conclusions

1. Accurate experimental results of transient cavitation in a closed tube have been obtained. Significant interactions exist between the pipewall, the fluid and the vapor cavities.
2. Transient tensile stresses of water and Poisson coupling induced cavitation can be measured accurately in the present apparatus.
3. The numerical model proposed by Tijsseling and Lavooij (1989) is sufficiently accurate if the flow is column separation dominant.
4. The proposed concentrated cavity—fluid/structure interaction model predicts the phenomenon with sufficient accuracy for most practical purposes. It can even simulate transient cavitation induced by radial expansions of pipewalls.

Acknowledgment

Delft Hydraulics is thanked for financially supporting the cavitation experiments at the University of Dundee.

References

Chaudhry, M. H., 1979, *Applied Hydraulic Transients*, Van Nostrand Reinhold, New York, ISBN 0-442-21517-7, pp. 276–281.

Davies, R. M., Trevena, D. H., Rees, N. J. M., and Lewis, G. M., 1955, "The Tensile Strength of Liquids Under Dynamic Stressing," *Proc. NPL Symp. on Cavitation in Hydrodynamics*, Paper 5, H. M. Stationery Office, London, UK.

Fox, J. A., and McGarry, M., 1983, "Pressure Transients in Pipelines Transporting Volatile Liquids," *Proc. 4th Int. Conf. on Pressure Surges*, Bath, UK: 21–23 Sept., BHRA, Cranfield, UK, pp. 39–57.

Kot, C. A., and Youngdahl, C. K., 1978, "Transient Cavitation Effects in Fluid Piping Systems," *Nuclear Engineering and Design*, Vol. 45, pp. 93–100.

Kranenburg, C., 1974, "Gas Release During Transient Cavitation in Pipes," *Proc. ASCE, J. Hyd. Div.*, Vol. 100, HY10, pp. 1383–1398.

Lavooij, C. S. W., and Tijsseling, A. S., 1989, "Fluid-Structure Interaction in Compliant Piping Systems," *Proc. 6th Int. Conf. on Pressure Surges*, Cambridge, UK: 4–6 Oct., BHRA, Cranfield, UK, pp. 85–100.

Martin, C. S., Padmanabhan, M., and Wiggert, D. C., 1976, "Pressure Wave Propagation in Two-Phase Bubbly Air-Water Mixtures," *Proc. 2nd Intl. Conf. on Pressure Surges*, London, UK: 22–24 Sept., BHRA, Cranfield, UK, paper C1.

Martin, C. S., 1983, "Experimental Investigation of Column Separation With Rapid Closure of Downstream Valve," *Proc. 4th Intl. Conf. on Pressure Surges*, Bath, UK: 21–23 Sept., BHRA, Cranfield, UK, Paper B3.

Plesset, M. S., 1969, "The Tensile Strength of Liquids," Fluids Engrg. and Appl. Mech. Conf., *Cavitation State of Knowledge*, Evanston, Ill.: 16–18 June, ASME, pp. 15–25.

Provoost, G. A., 1976, "Investigation Into Cavitation in a Prototype Pipeline Caused by Water Hammer," *Proc. 2nd Intl. Conf. on Pressure Surges*, London, UK: 22–24 Sept., BHRA, Cranfield, UK, Paper D2.

Safwat, H. H., 1972, "Photographic Study of Water Column Separation," *Proc. ASCE, J. Hyd. Div.*, Vol. 98, HY4, pp. 739–746.

Schwarz, W., 1978, "Druckstossberechnung unter Berucksichtigung der Radial-und Langsverschiebungen der Rohrwandung," Institut fur Wasserbau der Universitat Stuttgart, Mitteilungsheft 43, Stuttgart, Germany, ISBN 3-921694-43-4.

Schwirian, R. E., 1982, "Methods for Simulating Fluid-Structure Interaction and Cavitation With Existing Finite Element Formulations," Pressure Vessel and Piping Conf., *Fluid Transients and Fluid-Structure Interaction*, Orlando, Fla., 27 June–2 July, ASME, PVP-64, pp. 261–285.

Streeter, V. L., 1969, "Water Hammer Analysis," *Proc. ASCE, J. Hyd. Div.*, Vol. 95, HY6, pp. 1959–1972.

Tijsseling, A. S., and Lavooij, C. S. W., 1989, "Fluid-Structure Interaction and Column Separation in a Straight Elastic Pipe," *Proc. 6th Intl. Conf. on Pressure Surges*, Cambridge, UK: 4–6 Oct., BHRA, Cranfield, UK, pp. 27–41.

Tijsseling, A. S., and Lavooij, C. S. W., 1990, "Water Hammer With Fluid-Structure Interaction," *Applied Scientific Research*, Vol. 47, pp. 273–285.

Trevena, D. H., 1984, "Cavitation and the Generation of Tension in Liquids," *J. Physics D: Applied Physics*, Vol. 17, pp. 2139–2164.

Vardy, A. E., and Fan, D., 1986, "Water Hammer in a Closed Tube," *Proc. 5th Intl. Conf. on Pressure Surges*, Hannover, F. R. Germany: Sept. 22–24, BHRA, Cranfield, UK, Paper E3, pp. 123–137.

Vardy, A. E., and Fan, D., 1987, "Constitutive Factors in Transient Internal Flows," *Proc. NUMETA'87 Conf.*, Vol. 2, Swansea University, UK, Martinus Nijhoff, Netherlands, Paper T37.

Vardy, A. E., and Fan, D., 1989, "Flexural Waves in a Closed Tube," *Proc. 6th Intl. Conf. on Pressure Surges*, Cambridge, UK: 4–6 Oct., BHRA, Cranfield, UK, pp. 43–57.

Vliegenthart, A. C., 1970, "The Shuman Filtering Operator and the Numerical Computation of Shock Waves," *J. Engrg. Math.*, Vol. 4, No. 4, pp. 341–348.

Wiggert, D. C., Otwell, R. S., and Hatfield, F. J., 1985, "The Effect of Elbow Restraint on Pressure Transients," ASME JOURNAL OF FLUIDS ENGINEERING, Vol. 107, No. 3, pp. 402–406.

Wiggert, D. C., Lesmez, M. L., and Hatfield, F. J., 1987, "Modal Analysis of Fluid Vibrations in Liquid-Filled Piping Systems," *Symp. on Fluid Transients in Fluid-Structure Interaction*, Boston, MA, Dec. 13–18, ASME Winter Annual Meeting, ASME FED-56, pp. 107–113.

Wilkinson, D. H., 1978, "Acoustic and Mechanical Vibrations in Liquid Filled Pipework Systems," *Proc. BNES Conf. on Vibrations in Nuclear Plant*, Keswick, UK.

Wylie, E. B., 1984, "Simulation of Vaporous and Gaseous Cavitation," ASME JOURNAL OF FLUIDS ENGINEERING, Vol. 106, pp. 307–311.

Zielke, W., Perko, H-D., and Keller, A., 1989, "Gas Release in Transient Pipe Flow," *Proc. 6th Intl. Conf. on Pressure Surges*, Cambridge, UK: 4–6 Oct., BHRA, Cranfield, UK, pp. 3–13.